Nuclear Engineering and Technology 53 (2021) 611–617

Contents lists available at ScienceDirect

Nuclear Engineering and Technology

journal homepage: www.elsevier.com/locate/net

Original Article

The mechanical and thermodynamic properties of α-$Na_3(U_{0.84(2)},Na_{0.16(2)})O_4$: A combined first-principles calculations and quasi-harmonic Debye model study

Haichuan Chen [a, b]

[a] Key Laboratory of Fluid and Power Machinery, Ministry of Education, PR China
[b] School of Electrical Engineering and Electronic Information, Xihua University, Sichuan, 610039, PR China

ARTICLE INFO

Article history:
Received 25 May 2020
Received in revised form
16 July 2020
Accepted 21 July 2020
Available online 24 August 2020

Keywords:
Trisodium uranate
Mechanical properties
Thermodynamic properties
The first-principles calculations
The quasi-harmonic Debye model

ABSTRACT

The mechanical properties of α-$Na_3(U_{0.84(2)},Na_{0.16(2)})O_4$ have been researched using the first-principles calculations combined with the quasi-harmonic Debye model. The obtained lattice parameters agree well with the published experimental data. The results of elastic constants indicate that α-$Na_3(U_{0.84(2)},Na_{0.16(2)})O_4$ is mechanically stable. The polycrystalline moduli are predicted. The results show that the α-$Na_3(U_{0.84(2)},Na_{0.16(2)})O_4$ exhibits brittleness and possesses obvious elastic anisotropy. The hardness shows that it can be considered a "soft material". Furthermore, the Debye temperature θ_D and the minimum thermal conductivity k_{min} are also discussed, respectively. Finally, the thermal expansion coefficient α, isobaric heat capacity C_P and isochoric heat capacity C_V are evaluated through the quasi-harmonic Debye model.

1. Introduction

Since the liquid metallic sodium can be used as the sole coolant in the liquid metal fast breeder reactor, sodium-cooled fast reactors are considered a promising option for the fourth-generation nuclear reactors [1,2]. However, for these reactors, a safety problem arises. If the stainless steel cladding breaks, sodium inadvertently enters and reacts with the (U, Pu)O_2 mixed oxide fuel. The potential reaction between Na and (U, Pu)O_2 mixed oxide fuel leads to the formation of Na_3(U, Pu)O_4, which we have written as Na_3MO_4 (M is U, Pu) for convenience [3]. Na_3MO_4 can only be studied in special glove-boxes due to it contains plutonium. The Na-O-U ternary systems had attracted a lot of attention due to the phase diagram is isomorphism with (U,Pu)-O-Na diagram, and have similar thermomechanical and thermodynamic properties of the Na_3UO_4 and $Na_3(U_{1-x},Pu_x)O_4$ [4–6]. In 1964, Scholder et al. [7] reported α-phase Na_3UO_4, which has a face-centered cubic (*fcc*) structure with a = 0.477 nm at room temperature. The U and Na atoms are randomly distributed throughout the cation position. At high temperature, Marcon et al. [8] reported a second *fcc* structure of Na_3UO_4 (γ-phase) with a lattice parameter of 9.56 Å. Bartram et al. [9] revealed a new structure at 973 K with a = 9.54 Å and the composition $Na_5U_{11}O_{16}$ (β-phase). However, the x-ray diffraction pattern of β-$Na_5U_{11}O_{16}$ contains many additional reflection lines. Lorenzelli et al. [10] pointed out that the correct composition is Na_3UO_4, and found a reversible phase transition between the γ phase and β phase at 1348 ± 25 K. O'hare [11] investigated the enthalpy of formations of α-Na_3UO_4. Fredrickson et al. [12] measured the enthalpy of Na_3UO_4 in the temperature range 298–1200 K using high-precision drop-calorimetric system. Hofman et al. [13] investigated the thermal expansion and thermal conductivity of Na_3UO_4. The results show that below 773 K, the compositional differences of the samples have a significant effect on thermal conductivity and thermal expansion. We have previously reported the mechanical and thermodynamic properties of cubic (α-phase) and orthorhombic phase of Na_3UO_4 (β-phase) [14]. However, as far as we known, no detailed studies for the elastic, hardness and some thermodynamic properties of α-$Na_3(U_{0.84(2)},Na_{0.16(2)})O_4$ have been reported except the crystal structure which is investigated by Smith and Illy et al. [15,16]. In view of these circumstances, in this work, we investigated those properties of α-$Na_3(U_{0.84(2)},Na_{0.16(2)})O_4$ by using the first-principles calculation combining with quasi-harmonic Debye model.

E-mail addresses: chenhaichuan@mail.xhu.edu.cn, haichuanchenxhedu@163.com.

https://doi.org/10.1016/j.net.2020.07.027

2. Calculation methods

In this work, all the first-principles calculations were executed using the ultrasoft pseudopotential plane-wave method [17]. The electronic exchange and correlation energy was tackled by the generalized gradient approximation (GGA) [18] parameterized by Perdew and his co-worker Burke and Ernzerhof [19]. The valence electron configurations are $2s^2 2p^4$ for O, $2s^2 2p^6 3s^1$ for Na and $5f^3 6s^2 6p^6 6d^1 7s^1$ for U. The *k*-points sampling integration over the first Brillouin zone was employed the Monkhorst-Pack method with 6 × 5 × 6 special *k*-point meshes, and the cutoff energy is 700 eV. The Broyden-Fletcher-Goldfarb-Shanno (BFGS) algorithm was used to optimize the ground state crystal structure [20–23].

3. Results and discussions

3.1. Cystals structure

The α-$Na_3(U_{0.84(2)},Na_{0.16(2)})O_4$ has monoclinic symmetry (space group *P*2/*c*, No. 13), which is isostructural with Na_3BiO_4 [15,16]. In α-$Na_3(U_{0.84(2)},Na_{0.16(2)})O_4$, the U and Na atom site in *2e* Wyckoff position with a ratio of U/Na = 42/8, three Na atom sites in *2e*, *2f* and *2f* Wyckoff position, respectively, and two O atom sites in *4g* position (Fig. 1). The calculated atomic positions and lattice parameter are listed in Table 1 and accompany with the published experimental data. It can be observed from Table 1 that the optimized lattice parameter are somewhat underestimated compare with experimental data and the difference are 0.53%, 0.71%, −0.27% and −0.34%, respectively, indicating that the calculation is reliable. Therefore, the optimized lattice parameter can be utilized to subsequent calculations.

3.2. Mechanical properties

The "stress-strain" method is used to calculate the elastic constants C_{ij}, which are bound up with the mechanical and dynamical behaviors of materials. The calculated C_{ij} for α-$Na_3(U_{0.84(2)},Na_{0.16(2)})O_4$ are tabulated in Table 1. The obtained results indicate that $C_{33}>C_{22}>C_{11}$, suggesting that α-$Na_3(U_{0.84(2)},Na_{0.16(2)})O_4$ should be more easily compressible along the *x* axis than the *y* and *z* axis. Furthermore, C_{44}, C_{55} and C_{66} are smaller than the C_{11}, C_{22} and C_{33}, indicating that α-$Na_3(U_{0.84(2)},Na_{0.16(2)})O_4$ is stiffer to compression strain than to shear strain. On the other hand, it is also worth to point out that C_{15}, C_{25}, C_{35} and C_{46} consist of a negative value. This is probably due to that α-$Na_3(U_{0.84(2)},Na_{0.16(2)})O_4$ single crystal is a highly anisotropic material. Finally, the magnitudes of C_{15}, C_{25}, C_{35} and C_{46} are smaller than others. If they were equal to 0, the crystal would have had an orthorhombic symmetry. It is a tough task to measure these four constants by the experiment because it requires accurate sound velocity measurements on high-quality homogeneous crystals with precise orientation. In this work, the value of C_{15}, C_{25}, C_{35} and C_{46} can be obtained by the first-principles calculations. Unfortunately, to the best of author's knowledge, there are no experimental and theoretical data to test our calculated. The obtained research results in this work could provide useful reference for future research.

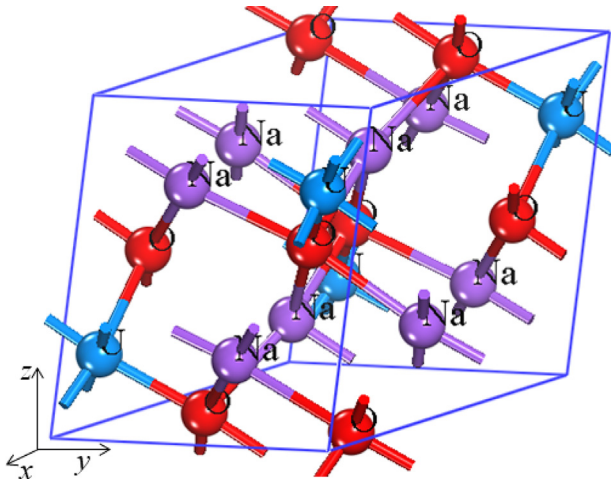

Fig. 1. The structure of α-$Na_3(U_{0.84(2)},Na_{0.16(2)})O_4$.

The mechanical stability of material requires that the strain energy be positive for any homogenous elastic deformation, which means that the independent C_{ij} should satisfy the generalized Born-Huang criterion [24,25]:

$$C_{46}^2 - C_{44}C_{66} > 0 \tag{1}$$

$$C_{11}C_{25}^2C_{33} - C_{13}^2C_{25}^2 + C_{15}^2g_1 + 2C_{12}C_{13}C_{25}C_{35} - 2C_{11}C_{23}C_{25}C_{35} - C_{12}^2C_{35}^2 + C_{11}C_{22}C_{35}^2 + 2C_{15}g_2 + C_{55}g_3 > 0 \tag{2}$$

$$g_1 = C_{22}C_{33} - C_{23}^2 \tag{3}$$

$$g_2 = C_{13}C_{23}C_{25} - C_{12}C_{25}C_{33} - C_{13}C_{22}C_{35} + C_{12}C_{23}C_{35} \tag{4}$$

$$g_3 = C_{13}^2C_{22} - 2C_{12}C_{13}C_{23} + C_{11}C_{23}^2 + C_{12}^2C_{33} - C_{11}C_{22}C_{33} \tag{5}$$

It can be found from Table 1 that the C_{ij} of α-$Na_3(U_{0.84(2)},Na_{0.16(2)})O_4$ satisfies the generalized Born-Huang criterion, meaning that it is mechanically stable.

Theoretically, the bulk modulus *B*, Young's modulus *E*, shear modulus *G* and Poisson's ratio σ of the polycrystalline material can be obtained from the independent C_{ij} of its monocrystalline phase. The Young's modulus *E* and Poisson's ratio σ can be calculated by Ref. [26,27]:

$$E = 9BG/(3B+G) \tag{6}$$

$$\sigma = (3B-2G)/(6B+2G) \tag{7}$$

Where $G = \frac{1}{2}(G_V + G_R)$, $B = \frac{1}{2}(B_V + B_R)$. G_V and B_V are Voigt bound of shear and bulk modulus, while the G_R and B_R are the Reuss bound of shear and bulk modulus, which can be calculated from the C_{ij} seen in Ref. [28]. The obtained results of the above polycrystalline modulus are given in Table 1. The *B* of α-$Na_3(U_{0.84(2)},Na_{0.16(2)})O_4$ (62.2 GPa) is 51.9% lower than the *c*-Na_3UO_4 (119.9 GPa) [14]. The result indicates that *c*-Na_3UO_4 is incompressibility than α-$Na_3(U_{0.84(2)},Na_{0.16(2)})O_4$. The calculated of *G* and *E* is 36.0 GPa and 90.4 GPa, respectively, which is smaller than that of *o*-Na_3UO_4 (44.8 GPa and 108.8 GPa) and *c*-Na_3UO_4 (60.2 GPa and 154.8 GPa) [14]. The results show that α-$Na_3(U_{0.84(2)},Na_{0.16(2)})O_4$ can withstand lower shear stress and lower stiff than *o*-Na_3UO_4 and c-Na_3UO_4.

In materials science, ductility is the ability of a solid material to deform under tensile stress. When the material is stressed, if it is brittle, it will break without significant deformation. According to the Pugh criterion, If $B/G > 1.75$, the material behaves as ductileness, or else, the material exhibits brittleness [29]. Poisson's ratio σ, as a criterion for brittleness and toughness of material, has proved to be valuable over the years. Depending on Frantsevich's work, the critical value of the brittle-ductile transition of the material is σ=0.33 [30]. Furthermore, Pettifor indicated that a positive Cauchy pressure C_p demonstrates the damage tolerance and ductility of the

Table 1
Calculated structure parameters of α-$Na_3(U_{0.84(2)},Na_{0.16(2)})O_4$ together with the experimental data.

Materials	Space group	Lattice (Å)		Wykoff coordinates			
		Cal	Exp		Cal	Exp	Occ
α-$Na_3(U_{0.84(2)},Na_{0.16(2)})$	*P2/c*	*a=5.861*	*a=5.892*	U	0,0.1366,0.25	0,0.1360,0.25	0.838
		b=6.724	*b=6.772*	Na	0,0.1366,0.25	0,0.1360,0.25	0.162
		c=5.932	*c=5.916*	Na	0,0.6129,0.25	0,0.6239,0.25	1
		β(°)		Na	0.5,0.8854,0.25	0.5,0.8692,0.25	1
		111.027	110.65	Na	0.5,0.4057,0.25	0.5,0.3996,0.25	1
				O	0.206,0.0981,-0.0015	0.2063,0.0959,-0.0066	1
				O	0.2339,0.3479,0.4683	0.2313,0.3494,0.4652	1

material, while a negative one shows the brittleness of the material [31]. For α-$Na_3(U_{0.84(2)},Na_{0.16(2)})O_4$, the C_p in the three lattice directions can be expressed as: $P_x = C_{23} - C_{44}$, $P_y = C_{13} - C_{55}$ and $P_z = C_{12} - C_{66}$. The calculated B/G, σ and Cauchy pressures P_x,P_y,P_z are 1.73, 0.258, 3.7 GPa, −2.2 GPa and −0.2 GPa, respectively. From the above, it can be clearly shown that α-$Na_3(U_{0.84(2)},Na_{0.16(2)})O_4$ is brittle in nature.

To further discussion the stiffness of the α-$Na_3(U_{0.84(2)},Na_{0.16(2)})O_4$, we predicted its Vickers hardness H_v. In the past few decades, based on various correlations between hardness and other physical parameters of material, a series of semi-empirical methods had been widely used to predict the hardness of materials. Among of them, linear correlations between H_v and B or G were widespread utilized. However, the simple linear relationship does not really suit all materials. Recently, two kinds of semi-empirical model had been proposed by Chen et al. [32] and Ozisik et al. [33]. They found that the H_v of material can be expressed as:

$$H_v^k = 2\left(k^2G\right)^{0.585} - 3, k = G\Big/B \tag{8}$$

$$H_v^\sigma = \frac{(1-2\sigma)^E}{6(1+\sigma)} \tag{9}$$

In order to calculate the H_v of α-$Na_3(U_{0.84(2)},Na_{0.16(2)})O_4$, the above two semi-empirical models are applied and the results are summarized in Table 1. We can find from this Table that the value of H_v^k (5.6 GPa) is in accordance with the value of H_V^σ (5.8 GPa), and we also found that the value of α-$Na_3(U_{0.84(2)},Na_{0.16(2)})O_4$ is lower than that of *c*-Na_3UO_4 (8.63 GPa) and *o*-Na_3UO_4 (8.54 GPa). We can conclude that it can be considered a "soft material".

3.3. Quantification of the anisotropy

Anisotropic behavior reflects the properties of bonds in different directions, and a proper description of this anisotropic behavior plays an important role in industrial applications as well as crystal physics. To investigate the anisotropic properties, several criteria have been proposed by the pioneering scientist. Among of them, the three-dimensional (3D) surface of the bulk and Young's modulus are effective method to characterize the anisotropy of the material along its crystal directions.

For α-$Na_3(U_{0.84(2)},Na_{0.16(2)})O_4$, the 3D surfaces for B and E can be obtained [34]:

$$B^{-1} = \left(s_{11}+s_{12}+s_{13}\right)l_1^2 + \left(s_{12}+s_{22}+s_{23}\right)l_2^2 + \left(s_{13} + s_{23}+s_{33}\right)l_3^2 + \left(s_{15}+s_{25}+s_{35}\right)l_1l_3 \tag{10}$$

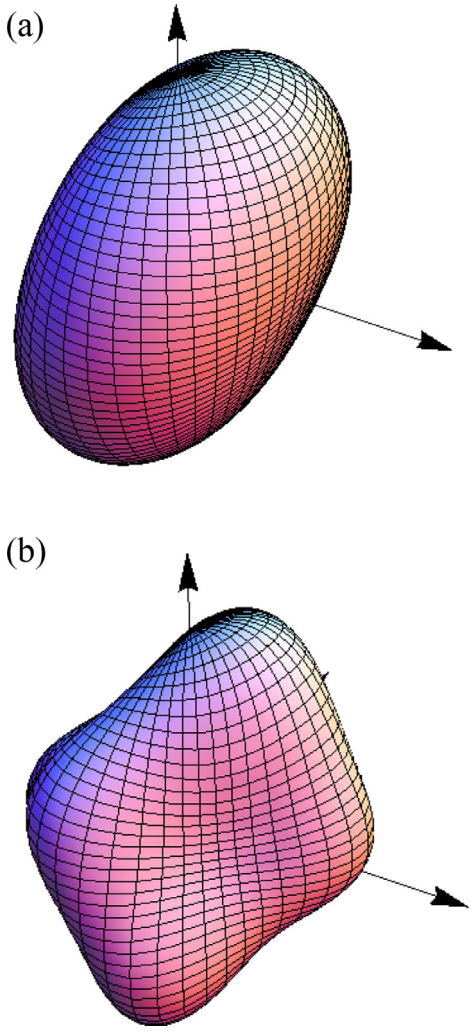

Fig. 2. 3D directional dependence of the B and E of α-$Na_3(U_{0.84(2)},Na_{0.16(2)})O_4$: (a) bulk modulus, (b) Young's modulus.

$$E^{-1} = l_1^4s_{11} + 2l_1^2l_2^2s_{12} + 2l_1^2l_3^2s_{13} + 2l_1^3l_3s_{15} + l_2^4s_{22} + 2l_2^2l_3^2s_{23} + 2l_1l_2^2l_3s_{25} + l_3^4s_{33} + 2l_1l_3^3s_{35} + l_2^2l_3^2s_{44} + 2l_1l_2^2l_3s_{46} + l_1^2l_3^2s_{55} + l_1^2l_2^2s_{66} \tag{11}$$

Where s_{ij} are the elastic compliance constants, l_1,l_2 and l_3 are the directional cosines.

The 3D surfaces of B and E are plotted in Fig. 2 (a) and (b), respectively. It can be seen from Fig. 2 that the 3D surfaces of B and

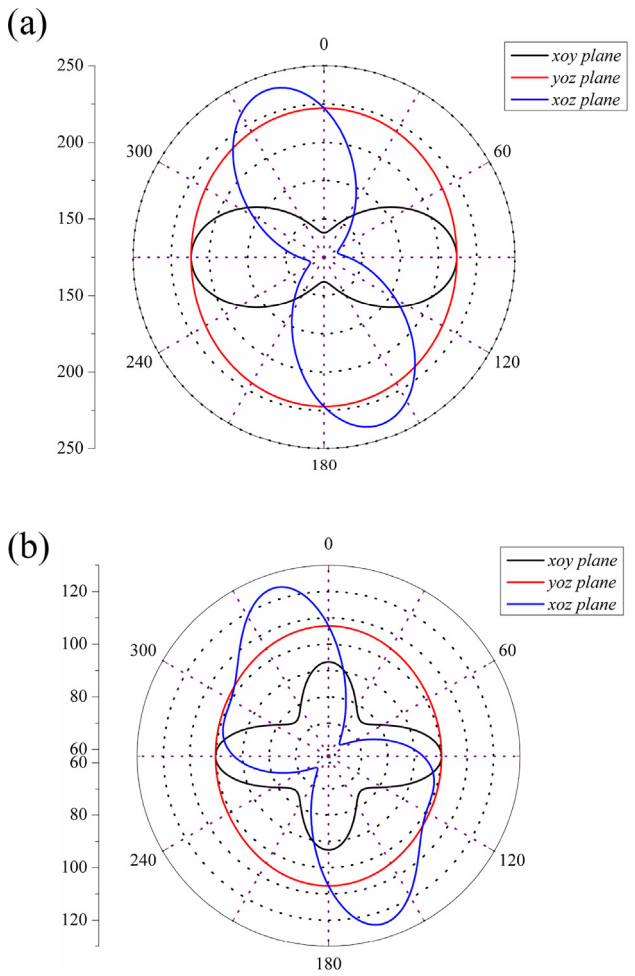

Fig. 3. The cross-sections of B and E of α-$Na_3(U_{0.84(2)},Na_{0.16(2)})O_4$ on the *xoy*, *yoz* and *xoz* plane: (a) bulk modulus, (b) Young's modulus.

E are obviously deviate from the spherical shape, meaning that the α-$Na_3(U_{0.84(2)},Na_{0.16(2)})O_4$ possesses obvious elastic anisotropy. From Fig. 2(a), we can also see that the B_x=140.9 GPa, B_y=212.0 GPa and B_z=222.4 GPa. With the aim of getting a better insight into the anisotropic features, the cross-section of the above surfaces on the *xoy*, *yoz* and *xoz*-planes are plotted in Fig. 3 (a) and (b), respectively.

From Fig. 3(a), for the *xoy* plane, the maximum bulk modulus B_{max} is 212.0 GPa and the minimum bulk modulus B_{min} is 140.9 GPa, and the ratio of B_{max}/B_{min} = 1.50. For the *yoz* plane, B_{max} is

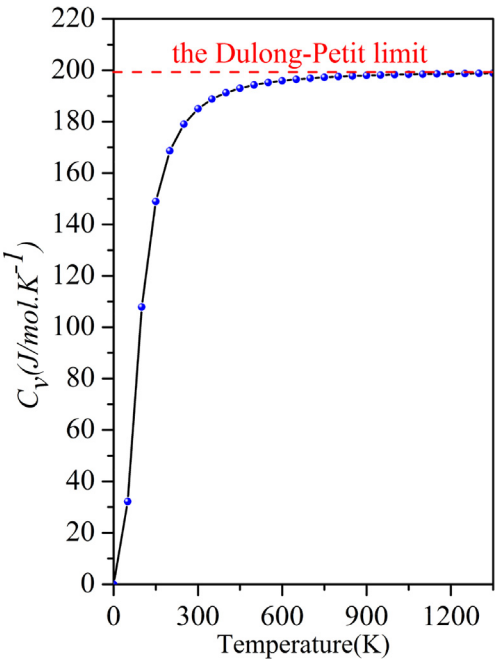

Fig. 4. The C_v of α-$Na_3(U_{0.84(2)},Na_{0.16(2)})O_4$ as functions of temperature.

222.4 GPa, B_{min} is 212.0 GPa, and the B_{max}/B_{min} = 1.05. For the *xoz* plane, B_{max} is 240.3 GPa, B_{min} is 134.5 GPa, and the B_{max}/B_{min} = 1.79. One can see that the B exhibits less anisotropy in the *yoz* plane compared to the *xoy* and *xoz* planes. The cross-sections of E on the *xoy*, *yoz* and *xoz* plane are depicted in Fig. 3(b). From Fig. 3(a), the minimum value of E_{min} is 75.5 GPa which is deviated by 43° from the x axis towards the y axis, and the maximum of E_{max} is 100.3 GPa at the y axis, the E_{max}/E_{min} = 1.33. For the *yoz* plane, the E_{max} is 106.9 GPa at z axis, and the E_{min} is 100.03 GPa at y axis, and the E_{max}/E_{min} = 1.07. For the *xoz* plane, the E_{min} is 63.6 GPa which is deviated by 43° from the z axis towards the x axis, and the E_{max} is 124.6 GPa at the y axis, the E_{max}/E_{min} = 1.96. So, we can conclude that the E of the *xoz*-plane has a bigger anisotropic than the others. Finally, the E_x = 93.3 GPa, E_y = 100.3 GPa and E_z = 106.9 GPa.

3.4. Thermodynamic properties

The Debye temperature θ_D can be estimated through the following equations [35]:

Table 2
Calculated C_{ij}, B, G, E, H_V, B/G, σ, v_l, v_t, θ_D and k_{min} of α-$Na_3(U_{0.84(2)},Na_{0.16(2)})O_4$.

Single crystal elastic constants			Polycrystalline elastic modulus			Thermodynamic properties		
C_{11}	104.6	GPa	B_V	63.1	GPa	v_t	2651	m/s
C_{22}	124.0	GPa	B_R	61.3	GPa	v_l	4640	m/s
C_{33}	133.2	GPa	B_H	62.2	GPa	θ_D^e	367	K
C_{44}	39.3	GPa	G_V	37.4	GPa	θ_D^q	376	K
C_{55}	33.1	GPa	G_R	34.5	GPa	K_{min}	0.71	$Wm^{-1}K^{-1}$
C_{66}	28.3	GPa	G_H	36.0	GPa			
C_{12}	28.1	GPa	E_V	93.7	GPa			
C_{13}	30.9	GPa	E_R	87.2	GPa			
C_{15}	6.9	GPa	E_H	90.4	GPa			
C_{23}	44.0	GPa	H_v^k	5.6	GPa			
C_{25}	−8.7	GPa	H_v^σ	5.8	GPa			
C_{35}	12.9	GPa	B/G	1.73				
C_{46}	−5.3	GPa	σ	0.258				

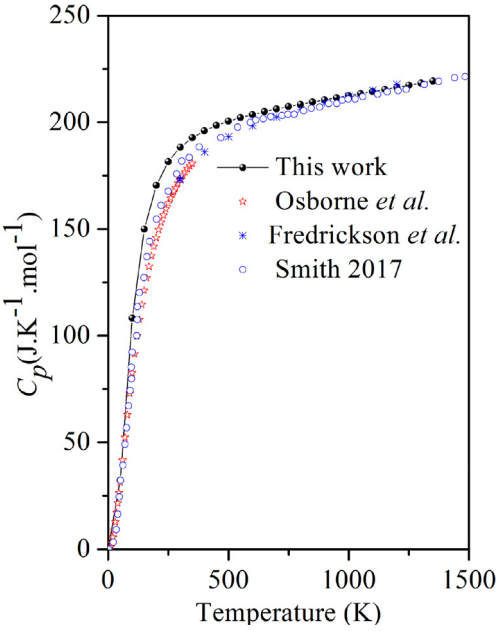

Fig. 5. The C_p of α-$Na_3(U_{0.84(2)},Na_{0.16(2)})O_4$ as functions of temperature.

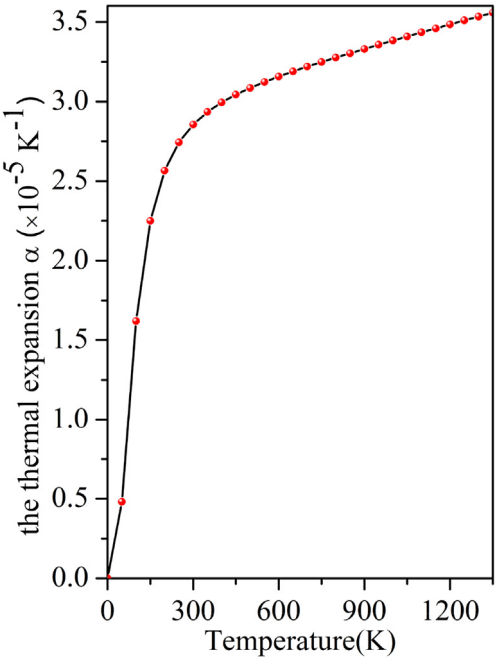

Fig. 7. The α of α-$Na_3(U_{0.84(2)},Na_{0.16(2)})O_4$ as functions of temperature.

$$\theta_D = \frac{h}{k_B}\sqrt[3]{\frac{3n}{4\pi}\left(\frac{N_A\rho}{M}\right)} \Big/ \sqrt{3\frac{1}{3}\left(\frac{2}{v_t^3}+\frac{1}{v_l^3}\right)} \tag{12}$$

Where $v_l = \sqrt{(3B+4G)/3\rho}$ is the longitudinal sound velocity, $v_t = \sqrt{G/\rho}$ is the transverse sound velocity, k_B is Boltzmann constant, h is Planck constant, N_A is Avogadro number, M is the molecular weight, ρ is the density and n is the number of atoms. The calculated v_l, v_t and θ_D of α-$Na_3(U_{0.84(2)},Na_{0.16(2)})O_4$ are gathered in Table 2. From Table 2, we can see that the θ_D is 367 K, which is smaller than that for *c*-Na_3UO_4 (453 K) and *o*-Na_3UO_4 (388 K) [14].

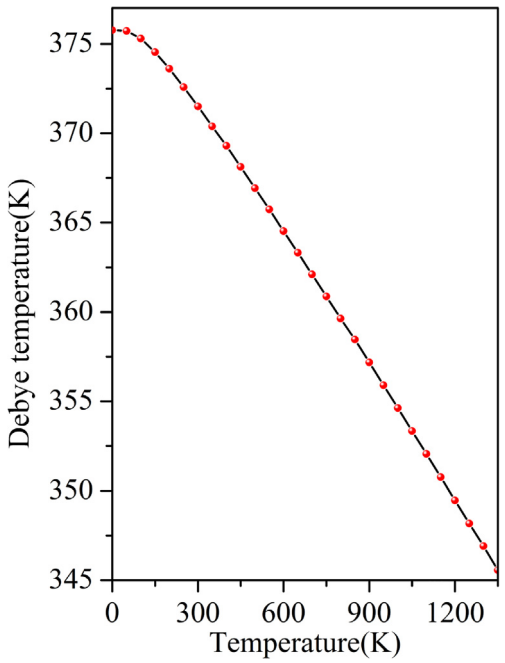

Fig. 6. The θ_D of α-$Na_3(U_{0.84(2)},Na_{0.16(2)})O_4$ as functions of temperature.

Generally speaking, a material with a higher θ_D means a higher thermal conductivity k_{min}. In order to predict the k_{min}, three theoretical methods had been proposed by Cahill's [36], Clarke [37,38] and Long et al. [39]. The k_{min} obtained from Long's model is about 30.2% and 19.6% lower than the one obtained from Cahill's and Clarke's model [40]. In this work, the k_{min} can be evaluated by Long and co-work's model [39]:

$$k_{min} = \left\{\frac{1}{3}\left[2(2+2\sigma)^{\frac{3}{2}} + \left(1-\frac{2\sigma^2}{1-\sigma}\right)^{\frac{3}{2}}\right]\right\}^{-\frac{1}{3}} k_B n^{\frac{2}{3}}\left(\frac{E}{\rho}\right)^{\frac{1}{2}} \tag{13}$$

The result of k_{min} is shown in Table 1. The k_{min} was predicted to be 0.71 W m^{-1}K^{-1}. Thereby, α-$Na_3(U_{0.84(2)},Na_{0.16(2)})O_4$ is suitable as a thermal insulating material.

In addition, to study the thermal expansion coefficient α, isobaric heat capacity C_P and isochoric heat capacity C_V, we used the quasi-harmonic Debye model implemented in the Gibbs program [41]. In this model the non-equilibrium Gibbs function $G^*(V;P,T)$ takes the form:

$$G^*(V;P,T) = E(V) + PV + A_{vib}(\theta_D;T) \tag{14}$$

Where $E(V)$ is the total energy of α-$Na_3(U_{0.84(2)},Na_{0.16(2)})O_4$, P, V and T corresponds to the pressure, volume and temperature, and $A_{vib}(\theta_D;T) = nk_BT\left[\frac{9}{8}\frac{\theta_D}{T} + 3\ln(1-e^{-\theta_D/T}) - D(\theta_D/T)\right]$ is the vibrational Helmholtz free energy, $D(\theta_D/T)$ represents the Debye integral.

$$\theta_D = \frac{\hbar}{k_B}\left[6\pi^2V^{1/2}n\right]^{1/3} f(\sigma)\sqrt{\frac{B_s}{M}} \tag{15}$$

$$B_s \cong B(V) = V\left(\frac{d^2E(V)}{dV_2}\right) \tag{16}$$

$$f\left(\sigma\right) = \left\{3\left[2\left(\frac{2}{3}\frac{1+\sigma}{1-2\sigma}\right)^{\frac{3}{2}} + \left(\frac{1}{3}\frac{1+\sigma}{1-\sigma}\right)^{\frac{3}{2}}\right]^{-1}\right\}^{\frac{1}{3}} \tag{17}$$

Where B_s is the adiabatic bulk modulus. Then minimized the non-equilibrium Gibbs function $\partial G^*(V;P,T)/\partial V|_{P,T} = 0$. Thus, the C_V, C_P and α are given by:

$$C_V = 3nk_B\left[4D(\theta_D/T) - \frac{3\theta_D/T}{e^{\theta_D/T}-1}\right] \tag{18}$$

$$C_P = C_V(1+\alpha\gamma T) \tag{19}$$

$$\alpha = \frac{\gamma C_V}{B_T V} \tag{20}$$

Fig. 4 presents the temperature-dependent behavior of the C_v. From this figure, at the temperatures lower than 300 K, C_v rapidly increases with increasing temperature (proportional to T^3) owing to the harmonic approximations of the Debye model, and increases slowly when T > 300 K. However, when temperatures higher than 900 K, the anharmonic approximations on C_v is suppressed and it nearly approaches to the Dulong-Pettit limit ($3nN_Ak_B \approx 199.38$ J $mol^{-1}.K^{-1}$).

The C_P of α-$Na_3(U_{0.84(2)},Na_{0.16(2)})O_4$ as functions of temperature is shown in Fig. 5. The experimental data measured of α-Na_3UO_4 at low temperatures (T < 350 K), at high temperatures (T > 300 K) and the theory values reported by Smith et al. are given for comparison. The values obtained are slightly overestimated less than 9% at the temperature from 200 K to 700 K. From Figs. 4 and 5, we can see that the C_v and C_p curves are very similar, and they are all proportional to T^3 at the temperature below 300 K. However, when T > 300 K, the C_p tends to an almost linear increase with increasing temperature.

The θ_D as a function of temperature is plotted in Fig. 6. At temperatures below 50 K, the θ_D is nearly constant and above 100 K, θ_D decreases linearly with increasing temperature. At 0 GPa and 0 K, the calculated θ_D is 376 K agree with the value (367 K) obtained by using the C_{ij}.

The effect of temperature on α of α-$Na_3(U_{0.84(2)},Na_{0.16(2)})O_4$ is depicted in Fig. 7. From Fig. 7, it is shown that the α increases sharply with the increase of temperature up to 300 K. Above 300 K, the α is nearly gradually approaches to a linear increase with increasing temperature due to the electronic contributions.

4. Conclusions

In summary, in this work, the elastic, Vickers hardness, anisotropic and thermodynamic properties of α-$Na_3(U_{0.84(2)},Na_{0.16(2)})O_4$ have been investigated by first-principles calculations. The obtained lattice parameters agree with the published experimental data. The C_{ij} and polycrystalline elastic properties are predicted. In addition, the θ_D and k_{min} are discussed, respectively. Finally, the C_V, C_P and α are also evaluated successfully through the quasi-harmonic Debye model. Unfortunately, as far as we known, there are no theoretical and experimental data related to these properties in the literature. Our work is a first to qualitatively predict of these properties of α-$Na_3(U_{0.84(2)},Na_{0.16(2)})O_4$ and the results can provide a useful reference for future research.

Declaration of competing interest

This paper is a new one. No conflict of interest exists in the submission of this manuscript, and manuscript is approved by all authors for publication. I would like to declare on behalf that the work described was original research that has not been published previously, and not under consideration for publication elsewhere, in whole or in part. All the authors listed have approved the manuscript that is enclosed.

Appendix A. Supplementary data

Supplementary data related to this article can be found at https://doi.org/10.1016/j.net.2020.07.027.

References

[1] K. Aoto, P. Dufour, H.Y. Yang, J.P. Glatz, Y. Kim, Y. Ashurko, R. Hill, N. Uto, A summary of sodium-cooled fast reactor development, Prog. Nucl. Energy 77 (2014) 247–265.
[2] H. Ohshima, S. Kubo, Sodium-cooled fast reactor, in: Igor L. Pioro (Ed.), Handbook of Generation IV Nuclear Reactors, Woodhead Publishing, Elsevier, Duxford, UK, 2016, pp. 98–118.
[3] G.L. Hofman, J.H. Bottcher, J.A. Buzzell, G.M. Schwartzenberger, Thermal conductivity and thermal expansion of hot-pressed trisodium uranate (Na_3UO_4), J. Nucl. Mater. 139 (1986) 151–155.
[4] M.G. Adamson, M.A. Mignanelli, P.E. Potter, M.H. Rand, On the oxygen thresholds for the reactions of liquid sodium with urania and urania-plutonia solid solutions, J. Nucl. Mater. 97 (1981) 203–212.
[5] M.A. Mignanelli, P.E. Potter, An investigation of the reaction between sodium and hyperstoichiometric urania, J. Nucl. Mater. 114 (1983) 168–180.
[6] M.A. Mignanelli, P.E. Potter, The reactions of sodium with urania, plutonia and their solid solutions, J. Nucl. Mater. 130 (1985) 289–297.
[7] R. Scholder, H. Gläser, Über Lithium- und Natriumuranate(V) und über strukturelle Beziehungen zwischen den Verbindungstypen Li_7AO_6 und Li_8AO_6, Z. Anorg. Allg. Chem. 327 (1964) 15–27.
[8] J.P. Marcon, O. Pesme, M. France, Rev. Int. Hautes Temp. Refract. 9 (1972) 193–196.
[9] S.F. Bartram, R.E. Fryxell, Preparation and crystal structure of $NaUO_3$ and $Na_{11}U_5O_{16}$, J. Inorg. Nucl. Chem. 32 (1970) 3701–3706.
[10] R. Lorenzelli, T. Athanassiadis, R. Pascard, Chemical reactions between sodium and $(U,Pu)O_2$ mixed oxides, J. Nucl. Mater. 130 (1985) 298–315.
[11] P.A.G. O'Hare, W.A. Shinn, F.C. Mrazek, A.E. Martin, Thermodynamic investigation of trisodium uranium(V) oxide (Na_3UO_4) I. Preparation and enthalpy of formation, J. Chem. Thermodyn. 4 (1972) 401–409.
[12] D.R. Fredrickson, P.A.G. O'Hare, Enthalpy increments for α- and β-Na_2UO_4 and Cs_2UO_4 by drop calorimetry the enthalpy of the α to β transition in Na_2UO_4, J. Chem. Thermodyn. 8 (1976) 353–360.
[13] G.L. Hofman, J.H. Bottcher, J.A. Buzzell, G.M. Schwartzenberger, Thermal conductivity and thermal expansion of hot-pressed trisodium uranate (Na_3UO_4), J. Nucl. Mater. 139 (1986) 151–155.
[14] H.C. Chen, W.Y. Tian, First-principles investigation of the physical properties of cubic and orthorhombic phase Na_3UO_4, Physica B 524 (2017) 144–148.
[15] A.L. Smith, P.E. Raison, L. Martel, D. Prieur, T. Charpentier, G. Wallez, E. Suard, A.C. Scheinost, C. Hennig, P. Martin, K.O. Kvashnina, A.K. Cheetham, R.J.M. Konings, A new look at the structural properties of trisodium uranate Na_3UO_4, Inorg. Chem. 54 (7) (2015) 3552–3561.
[16] M.-C. Illy, A.L. Smith, G. Wallez, P.E. Raison, R. Caciuffo, R.J.M. Konings, Thermal expansion of the nuclear fuel-sodium reaction product $Na_3(U_{0.84(2)},Na_{0.16(2)})O_4$ - structural mechanism and comparison with related sodium-metal ternary oxides, J. Nucl. Mater. 490 (2017) 101–107.
[17] J.P. Perdew, A. Ruzsinszky, G.I. Csonka, O.A. Vydrov, G.E. Scuseria, L.A. Constantin, X.L. Zhou, K. Burke, Restoring the density-gradient expansion for exchange in solids and surfaces, Phys. Rev. Lett. 100 (2008) 136406.
[18] B. Sadigh, A. Kutepov, A. Landa, P. Söderlind, Assessing relativistic effects and electron correlation in the actinide metals Th to Pu, Appl. Sci. 9 (2019) 5020.
[19] J.P. Perdew, K. Burke, M. Ernzerhof, Generalized gradient approximation made simple, Phys. Rev. Lett. 77 (1996) 3865–3868.
[20] C.G. Broyden, The convergence of a class of double-rank minimization algorithms 2. The new algorithm, J. Inst. Maths. Appl. 6 (1970) 222–231.
[21] R. Fletcher, A new approach to variable metric algorithms, Comput. J. 13 (1970) 317–322.
[22] D. Goldfarb, A family of variable-metric methods derived by variational means, Math. Comput. 24 (1970) 23–26.
[23] D.F. Shanno, Conditioning of quasi-Newton methods for function minimization, Math. Comput. 24 (1970) 647–656.
[24] R.A. Cowley, Acoustic phonon instabilities and structural phase transitions, Phys. Rev. B 13 (1976) 4877–4885.
[25] M. Bom, K. Huang, Dynamical Theory of Crystal Lattices, Clarendon, Oxford, 1954.

[26] R. Hill, The elastic behaviour of a crystalline aggregate, Proc. Phys. Soc. 65 (1952) 349–354.
[27] H.C. Chen, J.C. Wei, Y.Q. Chen, W.Y. Tian, Theoretical investigation of the mechanical and thermodynamic properties of titanium pernitride under high temperature and high pressure, J. Alloys Compd. 726 (2017) 1179–1185.
[28] J.P. Watt, Hashin-Shtrikman bounds on the effective elastic moduli of polycrystals with monoclinic symmetry, J. Appl. Phys. 51 (1980) 1520.
[29] S.F. Pugh, XCII. Relations between the elastic moduli and the plastic properties of polycrystalline pure metals, Phil. Mag. 45 (1954) 823–843.
[30] G.N. Greaves, A.L. Greer1, R.S. Lakes, T. Rouxel, Poisson's ratio and modern materials, Nat. Mater. 10 (2011) 823–837.
[31] D.G. Pettifor, Theoretical predictions of structure and related properties of intermetallics, Mater. Sci. Technol. 8 (1992) 345, 329.
[32] X.Q. Chen, H.Y. Niu, D.Z. Li, Y.Y. Li, Modeling hardness of polycrystalline materials and bulk metallic glasses, Intermetallics 19 (2011) 1275–1281.
[33] H. Ozisik, E. Deligoz, K. Colakoglu, E. Ateser, The first principles studies of the MgB_7 compound: Hard material, Intermetallics 39 (2013) 84–88.
[34] J.F. Nye, Physical Properties of Crystals, Oxford University Press Inc., New York, 1985, p. 145.
[35] L. Anderson, A simplified method for calculating the Debye temperature from elastic constants, J. Phys. Chem. Solid. 24 (1963) 909–917.
[36] D.G. Cahill, S.K. Watson, R.O. Pohl, Lower limit to the thermal conductivity of disordered crystals, Phys. Rev. B 46 (1992) 6131.
[37] D.R. Clarke, Materials selection guidelines for low thermal conductivity thermal barrier coatings, Surf. Coating. Technol. 163–164 (2003) 67–74.
[38] D.R. Clarke, C.G. Levi, Materials design for the next generation thermal barrier coatings, Annu. Rev. Mater. Res. 33 (2003) 383–417.
[39] J.P. Long, C.Z. Shu, L.J. Yang, M. Yang, Predicting crystal structures and physical properties of novel superhard p-BN under pressure via first-principles investigation, J. Alloys Compd. 644 (2015) 638–644.
[40] W.Y. Tian, J.H. Cai, H.C. Chen, Theoretical study the electronic, elastic properties and thermodynamics properties of ternary phosphide $SrPt_6P_2$, J. Phys. Chem. Solid. 106 (2017) 10–15.
[41] M.A. Blanco, E. Francisco, V. Luaña, GIBBS: isothermal-isobaric thermodynamics of solids from energy curves using a quasi-harmonic Debye model, Comput. Phys. Commun. 158 (2004) 57–72.